On a Possibility of High-Resolution Neutron Diffraction Observation of Inconel 718 Substructure Phases

Pavol Mikula[1,a] and Vasyl Ryukhtin[1,b]

[1]*Nuclear Physics Institute CAS, 250 68 Řež, Czech Republic;*

[a]*mikula@ujf.cas.cz*, [b]*ryukhtin@ujf.cas.cz*

Abstract: A feasibility of using an unconventional high-resolution neutron diffraction three-axis setting for studies of substructure phases of some alloys is presented. The usefulness of the diffraction setting is documented on measurements of powder diffraction profiles of several samples of Inconel 718 alloy. Even though the measurement at the medium power research reactor is rather time consuming, together with the γ phase matrix, it was possible to distinguish portions of other phases γ' and γ'' corresponding to created precipitates which depending on percentage content could have a significant influence on material properties.

Keywords: Neutron diffraction; Inconel 718 alloy; Substructure phases; Experimental Analysis

1 Introduction

Polycrystalline Ni-based superalloys are one of the very frequently used materials for high temperature load-bearing applications due to their high mechanical strength and chemical resistance. When looking for good mechanical properties and corrosion resistance of the material at elevated temperatures, a Ni-based superalloy 718 (also known as Inconel 718) is widely used e.g. in gas turbines in jet engines. The excellent properties of the Inconel 718, namely, strength and ductility, result from a good combination of the phases [1-3]: γ phase matrix with the fcc crystal structure, the coherent γ'' phase precipitates with Ni3Nb composition and a tetragonal bct ($D0_{22}$) crystal superstructure. Then, less often a fcc crystal structure of γ' precipitates could be present. The precipitation of either γ' or γ'' is dependent on the concentration of Ti and Nb. Typically, Inconel 718 is used in applications carried out at medium temperature, because above 650 °C the thermodynamically stable δ-phase forms, with Ni3Nb composition and an orthorhombic crystal structure (at the expense of the γ'' phase) which degrades the mechanical properties of the material. The δ phase precipitates either at the grain boundaries or intragranular.

Thanks to their excellent properties, fabricating components of the Alloy 718 using additive manufacturing (AM) methods are very attractive for different applications because they provide large possibilities of design flexibility. The most usually used AM processes are the so-called powder bed fusion ones, which include the following methods: direct metal laser sintering (DMLS), electron beam melting (EBM), selective heat sintering (SHS), laser powder bed fusion (LPBF usually referred as selective laser melting, SLM), and selective laser sintering (SLS). In the LPBF method a laser source is utilized for melting and selectively fusing together metallic powders, which are spread on a moving plate when the designed component is built. In the LPBF method, processing parameters as the laser power, scanning speed, hatch spacing, and layer thickness, are the most influential ones when producing microstructure for particular metals/alloys. For the studies of the microstructure and determination of the individual phases in the material, conventional X-ray diffraction (XRD) and neutron diffraction are usually used. Namely, synchrotron XRD, providing the high flux,

is very important for indexing and quantifying different phases in low fractions in the material. However, it is well known that due to a low penetration of X-rays into the material (for low energies X-rays), XRD provides required information related to the surface of the studied samples. On the other hand, neutron diffraction can use much larger probed volumes when fighting with a relatively much lower flux and thus also with much longer measurement time. As a feasibility study, in this paper we introduce neutron powder diffraction results of several samples of Inconel 718 as obtained by unconventional high-resolution neutron diffraction method in order to identify some phases having very close lattice spacings to the matrix one.

2 Experimental procedure

The neutron diffraction experiment was carried out by a high-resolution three-axis setting as schematically shown in Fig. 1. Following the sketch shown in Fig. 1 (for small widths of the samples), a maximum resolution from this arrangement can be achieved for minimal dispersion of the whole system [4,5]. When treated in momentum space, it means that the orientation of the Δk momentum domains related to the monochromator and analyzer should be matched to that of the sample, and this can be achieved by proper radii of curvature of the bent perfect crystal (BPC) monochromator and analyzer. Thus, focusing in real and momentum space can be realized. Contrary to the conventional two axis diffractometer, the diffraction profiles with the three-axis set-up are obtained by rocking (step-by-step) the (BPC) analyzer situated on the third axis of the diffractometer and the neutron signal is registered by a point detector (see Fig. 1).

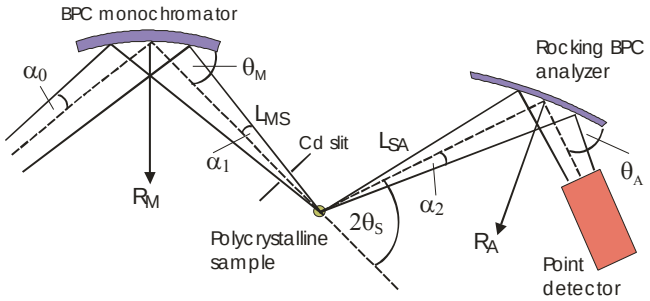

Fig. 1 Three-axis diffractometer setting employing BPC monochromator and analyzer as used in the experiment (R_M, R_A - radii of curvature, θ_M, θ_A - Bragg angles).

For $L_{MS}/(R_M \cdot \sin\theta_M) \neq 1$ and $L_{SA}/(R_A \cdot \sin\theta_A) \neq 1$, a general form for focusing in momentum space (not dependent on α_1 and α_2) which minimizes the dispersion between all elements can be derived as [6]

$$2\tan\theta_S = \tan\theta_M/(1 - L_{MS}/(R_M \cdot \sin\theta_M)) + \tan\theta_A/(1 - L_{SA}/(R_A \cdot \sin\theta_A)). \quad (1)$$

When fulfilling the condition (1), a maximum peak intensity and a minimum *FWHM* of the analyzer rocking curve can be expected. The experimental tests were carried out on the 3-axis neutron diffractometer installed at the Řež research reactor LVR-15. The diffractometer employs the Si(111)-monochromator and Si(311)-analyzer single crystals which have the dimensions of 200x40x4 mm^3 and 20x40x1.3 mm^3 (length x width x thickness), respectively. The monochromator Si(111) provides the neutron wavelength of 0.162 nm and has a fixed curvature with a radius R_M of about 12 m. The radius of curvature of the analyzer was

changeable in the range from 3.6 m to 36 m. It permitted us to determine an optimum analyzer curvature minimizing the dispersion and thus optimizing the resolution of the setting.

3 Experimental results

Examples of an excellent resolution of the 3-axis setting as documented by *FWHMs* of the analyzer rocking curves obtained on well annealed α-Fe(110) standard samples are shown in Fig. 2. Both samples were put on the second axis in the vertical position. High resolution of the setting points out an applicability of using it for studies of special material research tasks e.g. determination and volume content of different material phases, namely, when they have very close values of lattice spacing. Furthermore, microstructure analysis of plastically deformed samples, or samples under the external thermomechanical load during a deformation process, can be studied on the basis of diffraction profile analysis [7-10]. Recently, it has been found that the setting provides a sufficiently high resolution, though slightly relaxed, when wider slits (e.g. up to 20 mm) i.e. wider samples are used [11]. This phenomenon can be used e.g. for strain measurement on samples of large dimensions which is based on the measurement of the resulted peak shift $\Delta\theta_S$. When the sample of large dimensions is used, namely, its width introduces a too large resolution uncertainty in the case of the conventional two-axis strain/stress scanners.

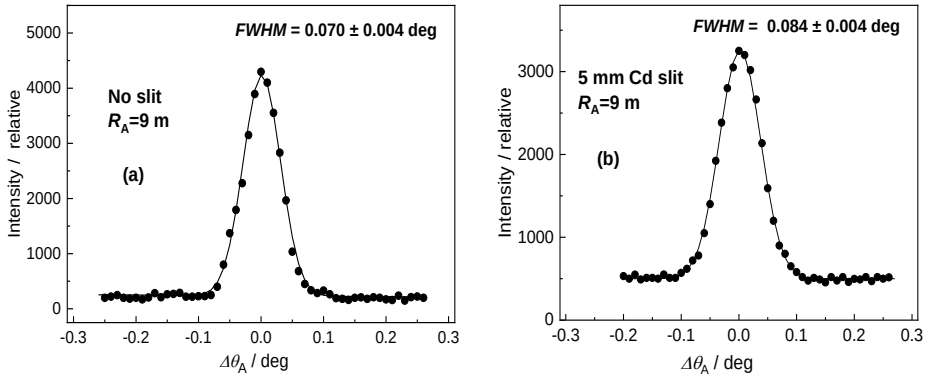

Fig. 2 α-Fe(110) diffraction profiles when using a well annealed 2 mm and a small steel plate of the dimensions of 2x7x15 mm^3 – (b).

Recently, it has been found out that the high-resolution setting can be used to distinguish diffraction profiles corresponding to very close lattice constants e.g. of different phases, as it is in the case of Inconel 718. For the measurement test we used several samples of Inconel 718 of the dimensions of 2x7x18 mm^3 which were put on the second axis vertically. The impinging beam on the sample was limited by a 5 mm Cd slit in order to be smaller than the width (7 mm) of the sample. Fig. 3 - Fig.5 show several results obtained on the wrought, SLM and wrought–aged samples which document the feasibility of the three-axis diffraction setting for such demanding experimental investigations. When using the values of the lattice spacings from ref. 3 and a simple formula $\Delta\theta_A \approx -\Delta(2\theta_S)$ valid for large values of R_A, our results well correspond to the ones obtained in ref. 1.

The inspection of Fig. 3 reveals that the main maximum (the red line) corresponds to the γ phase of the matrix while the small maxima at the shoulders correspond to the separated γ' (green line) and γ'' (blue line) phases, respectively. Then, Fig. 4 reveals that the main maximum (the red line) corresponds to the γ phase while the small maximum at the shoulder

(green line) corresponds to the γ' phase. On the other hand, Fig. 5 shows that together with the main γ phase, there is a considerable contribution of a mixture of γ' and γ'' phases (green line). The difference of the lattice spacings of the individual phase in the particular sample can be determined from the relation $\Delta\theta_A = (\Delta d_S/d_{0,S})\cdot\tan\theta_S$.

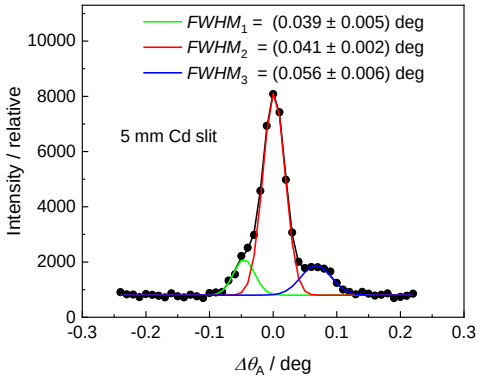

Fig. 3 Analyzer rocking curve related to the wrought Inconel 718 sample.

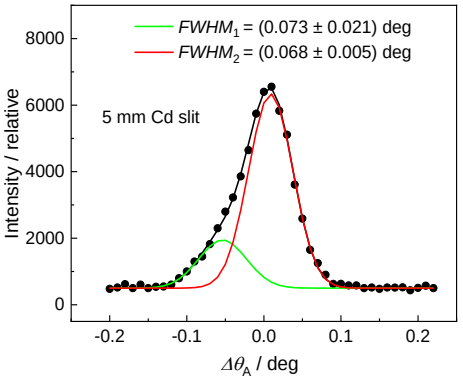

Fig. 4 Analyzer rocking curve related to the SLM Inconel 718 sample.

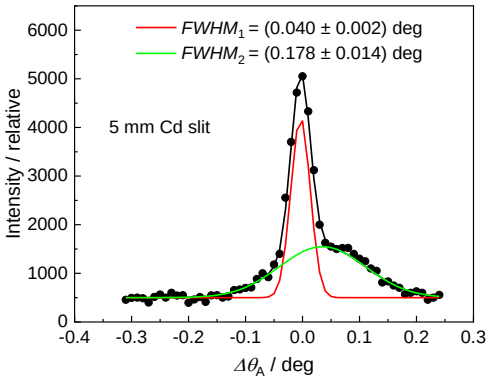

Fig. 5 Analyzer rocking curve related to the wrought-aged Inconel 718 sample.

Conclusion/Summary

High-resolution three-axis setting employing BPC Si(111) monochromator and BPC Ge(311) analyser with a polycrystalline sample between them was tested on the NPI neutron optics diffractometer and its feasibility of using it for investigation of special tasks of powder diffractometry was demonstrated. Namely, the excellent properties of the diffractometer setting permitted us to identify a substructure of Inconel 718 polycrystalline alloy containing several phases having close lattice spacings. As the mechanical properties considerably depend on the volume content of additional phases accompanying the main one their determination could be highly important. Naturally, the diffractometer setting could also be exploited for measurements of diffraction profiles of plastically deformed samples subjected e.g. to thermo-mechanical load and from their analysis to evaluate the dislocation density and a mean grain size in the polycrystalline sample. Of course, this setting can also be used for conventional macro-strain scanning based on the angular shifts $\Delta\theta_A$ of the obtained diffraction profiles, but due to the step-by-step analysis with the analyzer, rather time-consuming measurement could be impractical in comparison with the conventional

strain/stress diffractometer. We hope that the presented neutron diffraction setting can offer an additional support to complement the information achieved by using the other conventional characterization methodologies.

Acknowledgements

Measurements were carried out at the CANAM instrument of NPI CAS Řež installed the CICRR infrastructure, which is financially supported by the Ministry of Education and Culture - project LM2023041. The authors acknowledge support from ESS participation of the Czech Republic – OP (CZ.02.1.01/0.0/0.0/16_013/0001794) and from the project ESS Scandinavia-CZ II (LM2018111), respectively. Furthermore, they acknowledge support from the CAS in the frame of the program "Strategie AV21, No. 23". The authors thank B. Michalcová from NPI CAS for significant help with measurements and data elaborations.

References

[1] Čapek, J., Polatidis, E., Knapek, M., Lyphout, C., Casati, N., Pederson, R. and Strobl, M. "The effect of γ' and δ phase precipitation on the mechanical properties of Inconel 718 manufactu-red by selective laser melting: An in-situ neutron diffraction and acoustic emission study," *JOM* **73**, pp. 223-232 (2021).

[2] Solís, C., Munke, J., Bergner, M., Kriele, A., Mülbauer, M.J., Cheptiakov, D.V., Gehrmann, B., Rosler, J. and Gilles, R. "In-situ characterization at elevated temperatures of a new Ni-based superalloy VDM-780 Premium," *Metall Mater Trans A*, **49**, pp. 4373-4381 (2018).

[3] Repper, J. "Einfluss mikroskopischer Eigenspannungen auf die makroskopische Eigenspan-nungsanalyse mittels Neutronenbeugung," *PhD Thesis Technische Universität München*, 2010.

[4] Mikula, P., Šaroun, J., Ryukhtin, V. and Stammers, J. "An alternative neutron diffractometer performance for strain/stress measurements," *Powder Diffr*, **35**, pp. 185–189 (2020).

[5] Mikula, P., Šaroun, J. and Ryukhtin, V. "High-resolution residual strain/stress measurements on three-axis neutron diffractometer," *Adv Mat Res*, **1166**, pp. 33-40 (2021).

[6] Vrána, M., Lukáš, P., Mikula, P. and Kulda, J. "Bragg diffraction optics in high resolution strain measurements," *Nucl Instrum Meth A*, **338**, pp. 125-131 (1994).

[7] Delhez, R., De Keijser, T.H. and Mittemeijer, E.J. "Determination of crystallite size and lattice distortions through X-ray diffraction line profile analysis," *Fresenius' Zeitschrift für analytische Chemie*, **312**(1), pp. 1-16 (1982).

[8] Davydov, V., Lukáš, P., Strunz, P. and Kužel, R. "Single-line diffraction profile analysis method used for evaluation of microstructural parameters in the plain ferritic steel upon tensile straining," *Mater Sci Forum*, **571-572**, pp. 181-188 (2008).

[9] Macek, K., Lukáš, P., Janovec, J., Mikula, P. Strunz, P., Vrána, M. and Zaffagnini, M. "Austenite content and dislocation density in electron beam welds of a stainless maraging steel," *Materials Science and Engineering: A*, **208**, pp. 131-138 (1996).

[10] Hirschi, K., Ceretti, M., Lukáš, P., Ji, N., Braham, C. and Lodini, A. "Microstrain measurement in plastically deformed austenitic steel," *Texture Microstruct*, **33**, pp. 219-230 (1999).

[11] Mikula, P., Ryukhtin, V., Šaroun, J. and Strunz, P. "On possible high-resolution residual strain/stress measurements by three-axis neutron diffractometer," *Materials – MDPI*, **13**, pp. 5449-5455 (2020).